Chemical Physics Letters 647 (2016) 117–121

Contents lists available at ScienceDirect

Chemical Physics Letters

journal homepage: www.elsevier.com/locate/cplett

Magnetic circular dichroism of chlorofullerenes: Experimental and computational study

Petr Štěpánek[1], Michal Straka, Jaroslav Šebestík, Petr Bouř*

Institute of Organic Chemistry and Biochemistry, Academy of Sciences, Flemingovo náměstí 2, 16610 Prague, Czech Republic.

ARTICLE INFO

Article history:
Received 20 November 2015
In final form 19 January 2016
Available online 27 January 2016

ABSTRACT

Magnetic circular dichroism (MCD) spectra of $C_{60}Cl_6$, $C_{70}Cl_{10}$ and $C_{60}Cl_{24}$ were measured and interpreted using a sum-over-state (SOS) protocol exploiting time dependent density functional theory (TDDFT). Unlike for plain absorption, the MCD spectra exhibited easily recognizable features specific for each chlorinated molecule and appear as a useful tool for chlorofullerene identification. MCD spectrum of $C_{60}Cl_{24}$ was below 400 nm partially obscured due to scattering and low solubility. In all cases a finer vibrational structure of the electronic bands was observed at longer wavelengths. The TDDFT simulations provided a reasonable basis for interpretation of the most prominent spectral features.

1. Introduction

Chlorination of fullerenes leads to halogenated compounds that can conveniently be used in organic synthesis of more complex fullerene derivatives. Such materials promise many applications in biology and industry [1]. Fullerene derivatization is also important for their metabolic processing, which currently raises many security concerns (http://cordis.europa.eu/project/rcn/89325_en.html). The chlorination is performed with various agents including chlorine gas, PCl_5, VCl_4, $SbCl_5$, ICl, ICl_3, or $KICl_4$ [2,3]. According to the reaction conditions, multiple products may be formed and various addition patterns are possible. In addition, chlorofullerenes of the same stoichiometry sometimes form stable isomers [4]. For example, the Buckminster fullerene (C_{60}) chlorinates to compounds ranging from $C_{60}Cl_2$ up to $C_{60}Cl_{24}$, although not all of them are stable [4]. In the present study, we investigate the spectroscopy of magnetic circular dichroism (MCD) of selected derivatives as a method helpful in separation and identification of these compounds.

In general, determination of the composition of chlorinated fullerene mixture is difficult. Standard methods involve nuclear magnetic resonance (NMR), mass spectroscopy (MS), high-performance liquid chromatography (HPLC), and optical spectroscopy. Even a combination of such techniques, however, may not be sufficient for reliable analysis [3]. Limited solubility of some derivatives is often critical for the NMR measurements. Some species are unstable and may decompose in solution, at elevated temperatures, and due to irradiation by light [3].

The MCD spectroscopy detects a small difference in absorption of the left- and right-circularly polarized light in a presence of static magnetic field. Because the difference can be both positive and negative, the technique can inherently provide more easily decipherable information about the electronic and molecular structure than plain absorption [5–7]. Recently, modern implementations of the quantum-chemical expressions of MCD intensities [8,9], in particular within the density functional theory (DFT) framework, provide a handy tool for interpretation of the spectra and stimulate new applications of MCD spectroscopy [10–17].

For fullerenes, first MCD studies of C_{60} were published in late 80s and early 90s [18,19]. The fact that (unsubstituted) fullerenes provide very rich and characteristic MCD spectra has been confirmed recently [20]. In fact, MCD signal is specific both for fullerenes of different chemical formulae and isomers [20]. Similarly, distinct MCD signals were observed for endohedral fullerenes $La@C_{82}$, $La_2@C_{80}$ and $Sc_3N@C_{80}$ [21].

In the present study three model molecules, $C_{60}Cl_6$, $C_{70}Cl_{10}$ and $C_{60}Cl_{24}$, were synthesized, their absorption and MCD spectra measured, and the results are discussed on the basis of time dependent density functional theory (TDDFT). A computationally efficient sum over states (SOS) methodology [10,22] is used to simulate chlorofullerene MCD spectra. As discussed below, such TDDFT computations provide a reasonable basis for the experiment.

* Corresponding author.
E-mail address: bour@uochb.cas.cz (P. Bouř).
[1] Present address: NMR Research Group, Faculty of Science, University of Oulu, PO Box 3000, 90014 Oulu, Finland.

http://dx.doi.org/10.1016/j.cplett.2016.01.047
0009-2614/

2. Methods

The $C_{60}Cl_6$, $C_{70}Cl_{10}$ and $C_{60}Cl_{24}$ compounds were synthesized using previously published procedures as specified in the Supporting Information. Absorption and MCD spectra were measured at room temperature (~293 K) on a Jasco J-815 CD spectrometer equipped with a 1.4 T permanent magnet. Samples dissolved in 1,2-dichlorobenzene were placed in a 1 cm fused-silica cell, the scanning speed was 5 nm/min, detector response constant 32 s, and data pitch 0.05 nm. Presented data are averages of two accumulations. $C_{60}Cl_6$ concentrations ranged from 0.4 mg/ml to 0.0267 mg/ml, $C_{60}Cl_{24}$ was measured as a saturated solution (~0.15 μg/ml), and $C_{70}Cl_{10}$ was measured for 0.16 and 0.08 mg/ml.

For the theoretical modeling, $C_{60}Cl_6$, $C_{70}Cl_{10}$ and $C_{60}Cl_{24}$ molecular geometries (Figure 1) were optimized using the BP86 and B3LYP functionals, and standard def-TZVP and 6-311+G* basis sets. The polarizable continuum solvent model (PCM) [23] was used to account for the 1,2-dichlorobenzene environment. The GAUSSIAN 09 revision D.01 program [24] was used for the geometry optimization; some computations were also done in Turbomole 6.3.1 [25].

By default, electronic absorption spectra were calculated at the B3LYP/PCM/6-31G* level for the B3LYP/PCM/6-311+G* geometries using TDDFT [26] as implemented in the Gaussian and Turbomole programs. In a test a larger 6-31+G* basis set (Figure S1) provided within the experimentally accessible region very similar absorption and MCD intensities as 6-31G*; we use the 6-31G* basis set as default as it allows us to compute more excited states covering a larger interval of wavelengths than the larger 6-31+G* basis. A truncated (400 state) SOS expansion is used for the generation of MCD intensities. From the TDDFT expansion coefficients approximate excited states were used in a sum over states (SOS) formula for MCD as implemented in the Guvcde program [10,22] interfaced to Gaussian and Turbomole. Spectral intensities were generated with Gaussian bands 0.1 eV wide (full width at half height). Control MCD computations were also performed with the Dalton 2011 code [27] using the complex polarization propagator (CPP) variant of the response theory [15], which provided very similar intensities as the SOS method, but with much higher demands on the computational resources. The CPP curves were generated with 5 nm increments (i.e. irregular energy intervals), computing five points at once, the gamma width was set to 0.0046 hartree. Typically, the computations were run in parallel at 4–8 processors.

3. Results and discussion

3.1. Experimental spectra

Absorption and MCD spectra of $C_{60}Cl_6$, $C_{60}Cl_{24}$ and $C_{70}Cl_{10}$ are plotted in Figure 2, together with those of C_{60} and C_{70} obtained previously [20]. The 'bare' fullerenes were measured in a relatively transparent *n*-hexane down to ~200 nm. The chlorinated derivatives were not much soluble in it, and their spectra could be measured to ~300 nm only, due to the high absorption of the 1,2-dichlorobenzene solvent. The long-wavelength absorption threshold of $C_{60}Cl_6$ (weak signal starting at ~522 nm, a larger one at ~400 nm) is slightly higher if compared to C_{60} (cf. the first strong peak at 328 nm). In $C_{60}Cl_{24}$ the absorption range is not much changed in comparison with $C_{60}Cl_6$, but the intensity within 400–550 nm is increased and the bands are sharper. The chlorination of C_{70} to $C_{70}Cl_{10}$ brings similar effects for the shift of the strongest absorption (254 nm → 315 nm); however, within 300–650 nm the C_{70} molecule exhibits many weaker bands already, intensity of which is redistributed after the chlorination.

The MCD spectra (right hand side of Figure 2) show a larger variability and reveal presence of more electronic transitions (also with several vibrational components) than the absorption. Note also that the signal might slightly depend on experimental conditions; for C_{60}, for example, the '−−+' bands at 251, 324 and 334 nm found in *n*-hexane (Figure 2) exist in an Argon matrix [28], too, but an additional positive signal around 255 nm was found in the latter environment. For $C_{60}Cl_6$, there are two strong MCD positive bands at 360 and 396 nm, a negative signal going down to the 300 nm limit, and six weaker bands above 400 nm, alternating in MCD sign but approximately of the same magnitude. $C_{60}Cl_{24}$ exhibits strong positive bands at 410 and 469 nm, a negative one at 460 nm with clear vibrational substructure, and a 510 nm positive peak. The $C_{60}Cl_{24}$ MCD spectra below 400 nm might not be reliable because of the limited solubility and a high scattering of the sample.

The MCD pattern of $C_{70}Cl_{10}$ is again quite unique; the signal above 400 nm is much stronger than for $C_{60}Cl_6$, but there are fewer (about three) strong bands resolved. As for $C_{60}Cl_6$, a weak MCD $C_{70}Cl_{10}$ signal is apparent up to about 570 nm. An interesting effect of the $C_{70} \rightarrow C_{70}Cl_{10}$ chlorination is the sign inversion of the strongest MCD band (324 → 343 nm).

3.2. Simulated absorption and MCD spectra

Similarly as previously observed for unsubstituted fullerenes [20] the calculated absorption and MCD spectra (Figure 3) reasonably well reproduce the main experimental features in studied chlorofullerenes. For the $C_{60}Cl_6$ absorption, the computation predicts higher intensity above 320 nm if compared to C_{60}; for $C_{70}Cl_{10}$ the intensity in this region diminishes relative to C_{70}, although the fine vibrational pattern is obviously not reproduced at the static approximation.

The signs of the principal MCD bands are reproduced correctly, although detailed features differ and transition wavelengths are calculated too low. For $C_{60}Cl_6$, the MCD experimental main maxima at 360 and 396 nm are reproduced at 257 and 314 nm; a weaker negative band at 420 nm (exp.) is calculated at 341 nm. Above 450 nm the fine experimental structure is not simulated

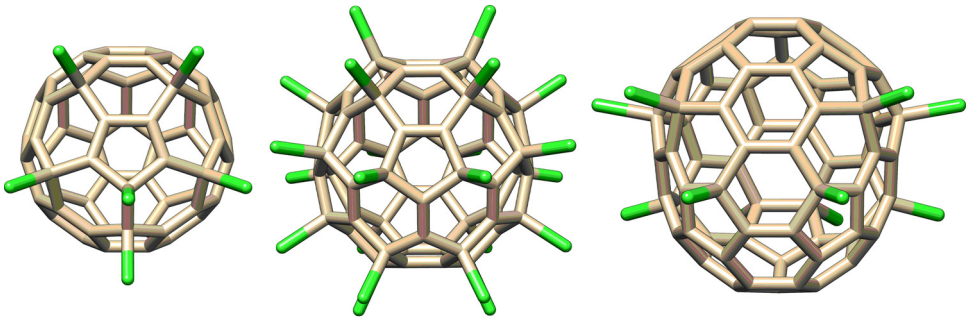

Figure 1. Optimized (B3LYP/CPCM/6-311++G**) $C_{60}Cl_6$, $C_{60}Cl_{24}$ and $C_{70}Cl_{10}$ geometries.

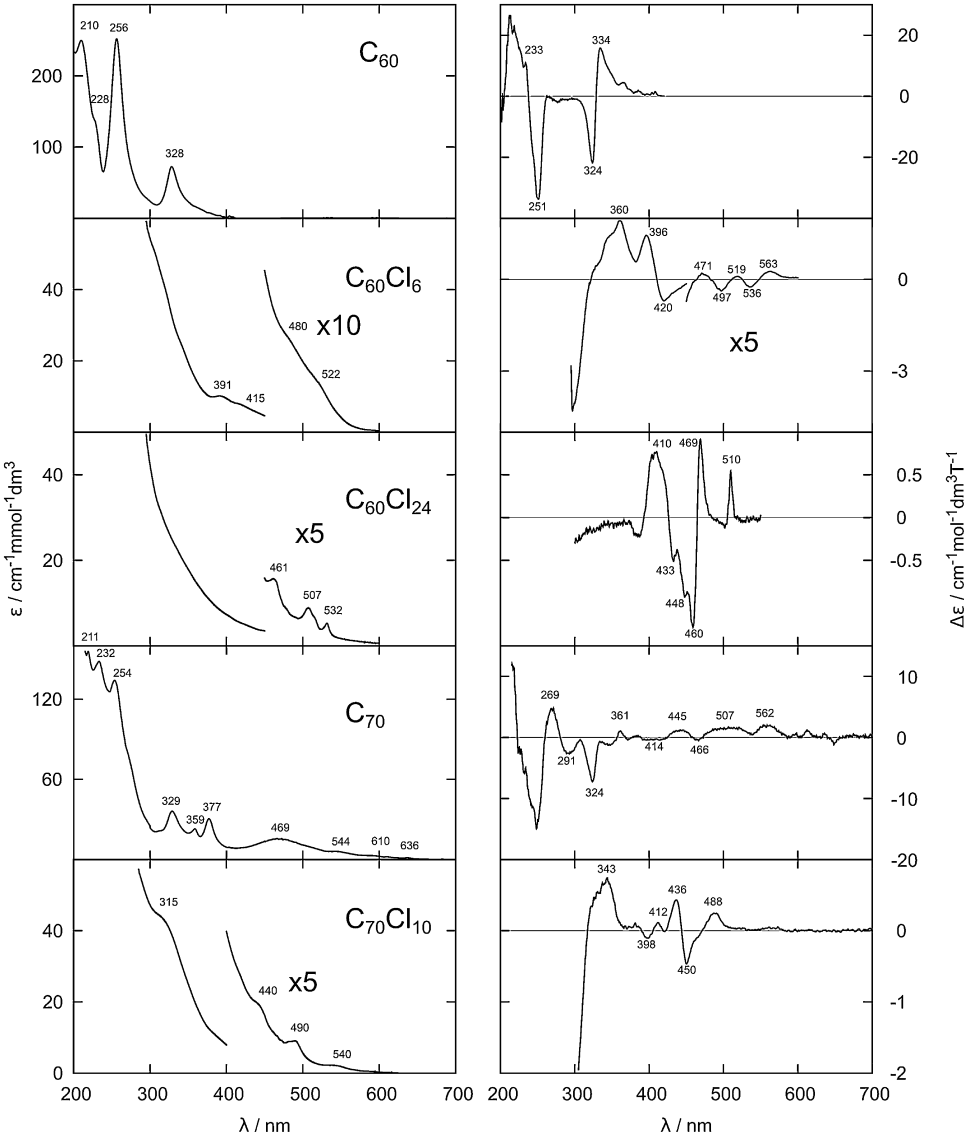

Figure 2. Experimental absorption (left) and MCD (right) spectra of C_{60}, C_{70}, and their $C_{60}Cl_6$, $C_{60}Cl_{24}$ and $C_{70}Cl_{10}$ derivatives, for 1,2-dichlorbenzene solutions. The intensity scale for $C_{60}Cl_{24}$ may not be reliable because of a low solubility. The C_{60} and C_{70} spectra were replotted from Ref. [20].

in detail; nevertheless this region contains 13 electronic transitions and we may suppose that vibronic interaction or DFT error is responsible for the too weak simulated signal here. We also calculated absorption contributions of the magnetic-dipole and electric-quadrupole transitions; these, however, are always about 1000× weaker than the electric-dipolar ones (Figure S2) and thus most probably cannot account for the observed MCD intensities. Similarly, for $C_{60}Cl_{24}$, the '+−++' feature at 410/460/469/510 nm is approximately visible in the calculation (241/294/323/338 nm), although the last two positive bands are not well pronounced. The '+−+−+' 343/398/436/450/488 nm $C_{70}Cl_{10}$ MCD bands seem to correspond to the 289/300/360/382/430 nm calculated ones.

To explore factors affecting computational accuracy, we investigated the effect of the geometry on spectral intensities. The equilibrium geometry of $C_{60}Cl_{24}$, for example, is reasonably-well reproduced by all the methods, with an average distance error smaller than 0.01 Å (Table S1). If equilibrium geometries calculated by different methods are used with the same level (B3LYP/6-31G*/PCM) for MCD computation, rather minor spectral changes (about 10% in intensities) are observed, although spectral bands are shifted by several nm (Figure S3). As another test of the sensitivity of the spectra to the geometry, the $C_{60}Cl_6$ geometry was distorted along the normal mode displacement of low-frequency vibrational modes, so that resultant energy change was close to the Boltzmann temperature quantum ($kT \sim 0.6$ kcal/mol). For three selected modes, the absorption and MCD spectra are plotted in Figure S4. One can see that the effect of such distortions on the spectra is rather minor, although MCD is more sensitive to them than the absorption. Only part of the inhomogeneous band broadening and minor spectral features can be explained by such geometry fluctuations.

Next, we investigate various theoretical formalisms used to generate MCD intensities. $C_{60}Cl_6$ spectra generated by the CPP [15] and SOS [10,22] methods are plotted in Figure 4. In addition, for SOS, both the length and gradient variants are shown. Unlike for smaller molecules [10], the gradient formalism seems to perform better than the length approach if compared to CPP, and also if compared to the present experimental result. This might be caused by incomplete basis set affecting in particular the magnetic dipole integrals [22] in the SOS MCD formula for the B-term [8,29]. Thus we find it most convenient to use the SOS/gradient method. Depending on implementation and computational parameters,

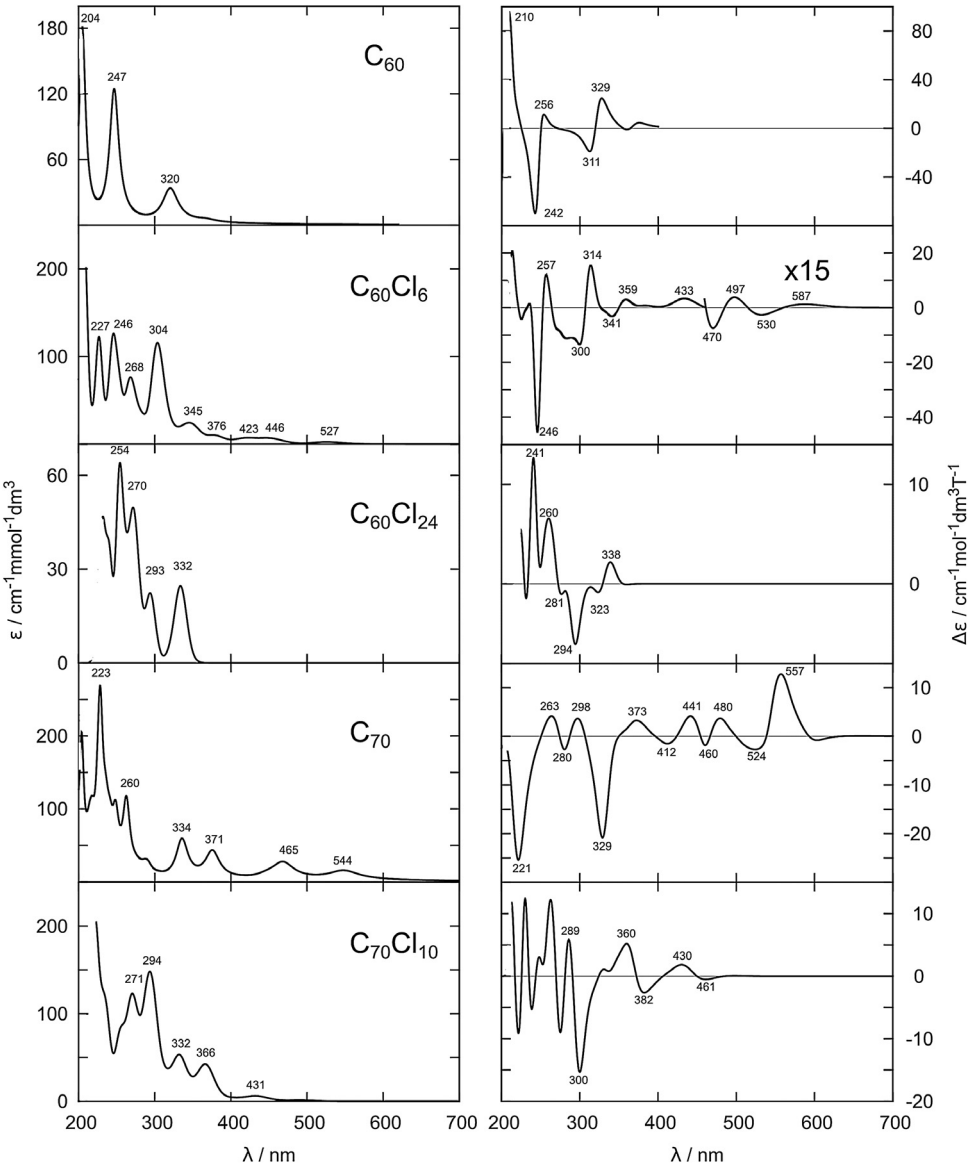

Figure 3. Calculated (B3LYP/CPCM/6-31G*) absorption (left) and MCD (right) spectra of C_{60}, C_{70}, and their $C_{60}Cl_6$, $C_{60}Cl_{24}$ and $C_{70}Cl_{10}$ derivatives. The C_{60} and C_{70} spectra were replotted from Ref. [20].

the SOS methodology may also be much faster than CPP (in our hands, the speed increased about 10-times), and allows stable computations with relatively large basis sets.

Much larger variations than for the MCD methodology appeared if different functionals were used; in Figures S5 and S6 spectra of $C_{60}Cl_6$ and $C_{60}Cl_{24}$ calculated with eight different functionals are shown. All the methods provide much better agreement with the experiment in transition frequencies for $C_{60}Cl_6$ than for $C_{60}Cl_{24}$, which suggest that the TDDFT methodology may fail for compounds containing too many chlorine atoms. For bare C_{60}, for example, the B3LYP and CAM-B3LYP functionals (cf. [20,30]) provided much closer MCD intensities than for $C_{60}Cl_6$ (Figure S5). For $C_{60}Cl_6$, some functionals, in particular those based on the general gradient approximation (GGA), such as PBE, provide rather unrealistic MCD patterns. Rather surprisingly, the functionals corrected for long-range interactions [31], CAM-B3LYP and wB97XD, do not give a good representation of the experiment. On the other hand, the more established B3LYP, PBE0, M06 and BP86 functionals provide at least somewhat similar MCD intensities, and thus suggest that the calculations may be reliable enough to guide interpretation of the most important experimental features.

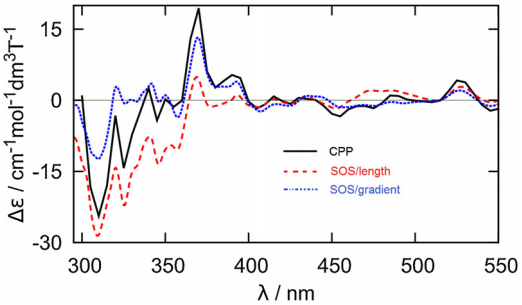

Figure 4. MCD $C_{60}Cl_6$ spectra generated by the CPP and SOS methods (BP86/6-31G*, vacuum).

One of desired improvements of the computational accuracy should also include the electronic–vibrational interactions. Proper account of the vibrational structures was already found important for many absorption and electronic circular dichroism spectra [32],

and latest study on small molecules suggest that it is important also for detail MCD interpretation [33]. This is currently connected with excessive computational demands for fullerenes, but presents a challenge for the future. The experimental data (e.g., Figure 2, [20]) suggest that these molecules have relatively rich and specific vibrational structure of the lowest-energy (longest-wavelength) transitions, similarly as for the underlying electronic MCD pattern discussed in the present study.

4. Conclusions

We synthesized three model chlorofullerene molecules, $C_{60}Cl_6$, $C_{70}Cl_{10}$, and $C_{60}Cl_{24}$, and measured and analyzed their MCD spectra to investigate the potential of this technique in resolution and characterization of functionalized fullerenes. Although rather unspecific variations were observed in the absorption, MCD spectra exhibited rich features characteristic for each molecule. The SOS–TDDFT simulations reproduced major features observed in experimental MCD spectra, but the comparison was somewhat hampered by the limited computational accuracy. Experimental difficulties (low solubility and scattering) were also encountered for $C_{60}Cl_{24}$. In spite of these problems, MCD spectroscopy appears as a very sensitive technique able to distinguish various structural features in fullerenes and their derivatives. The TDDFT computational methodology is certainly prone to future improvements. However, it enables one to understand the observed spectral features, and the possibility to simulate the spectra makes analytical MCD studies applicable more widely.

Acknowledgements

This work was supported by the Czech Science Foundation (No. 13-03978S and 14-03564S), Academy of Sciences (RVO-61388963) and Ministry of Education (CZ.1.05/3.2.00/08.0144).

Appendix A. Supplementary data

Supplementary data associated with this article can be found, in the online version, at doi:10.1016/j.cplett.2016.01.047.

References

[1] J.U. Franco, J.R. Ell, A.K. Hilton, J.C. Hammons, M.M. Olmstead, Fuller. Nanotub. Carbon Nanostruct. 17 (2009) 349.
[2] B.S. Razbirin, A.N. Starukhin, A.V. Chugreev, A.S. Zgoda, V.P. Smirnov, Y.S. Grushko, S.G. Kolesnik, P.F. Coheur, J. Lievin, R. Colin, Phys. Solid State 44 (2002) 2204.
[3] I.V. Kuvychko, A.V. Streletskii, N.B. Shustova, K. Seppelt, T. Drewello, A.A. Popov, S.H. Strauss, O.V. Boltalina, J. Am. Chem. Soc. 132 (2010) 6443.
[4] P.A. Troshin, O. Popkov, R.N. Lyubovskaya, Fuller. Nanotub. Carbon Nanostruct. 11 (2003) 165.
[5] W.R. Mason, A Practical Guide to Magnetic Circular Dichroism Spectroscopy, Wiley-Interscience, Portland, 2007.
[6] W. Voelter, R. Records, E. Bunnenberg, C. Djerassi, J. Am. Chem. Soc. 90 (1968) 6163.
[7] C. Djerassi, E. Bunnenberg, D.L. Elder, Pure Appl. Chem. 25 (1971) 57.
[8] P.J. Stephens, Adv. Chem. Phys. 35 (1976) 197.
[9] S. Coriani, P. Jørgensen, A. Rizzo, K. Ruud, J. Olsen, Chem. Phys. Lett. 300 (1999) 61.
[10] P. Štěpánek, P. Bouř, J. Comput. Chem. 34 (2013) 1531.
[11] E.I. Solomon, K.M. Light, L.V. Liu, M. Srnec, S.D. Wong, Acc. Chem. Res. 46 (2013) 2725.
[12] T. Kjaergaard, S. Coriani, K. Ruud, Wiley Interdiscip. Rev. Comput. Mol. Sci. 2 (2012) 443.
[13] M. Seth, T. Ziegler, in: R. VanEldik, J. Harley (Eds.), Advances in Inorganic Chemistry, Elsevier Academic Press, Inc., San Diego, 2010, p. 41.
[14] E.H. Marin, M. Seth, T. Ziegler, Inorg. Chem. 49 (2010) 6066.
[15] H. Solheim, K. Ruud, S. Coriani, P. Norman, J. Chem. Phys. 128 (2008) 094103.
[16] D. Ganyushin, F. Neese, J. Chem. Phys. 128 (2008) 114117.
[17] H. Solheim, L. Frediani, K. Ruud, S. Coriani, Theor. Chem. Acc. 119 (2008) 231.
[18] F. Negri, G. Orlandi, F. Zerbetto, Chem. Phys. Lett. 144 (1988) 31.
[19] M. Pilch, M. Pawlikowski, O.S. Mortensen, Chem. Phys. 172 (1993) 277.
[20] P. Štěpánek, M. Straka, V. Andrushchenko, P. Bouř, J. Chem. Phys. 138 (2013) 151103.
[21] M. Yamada, Z. Slanina, N. Mizorogi, A. Muranaka, Y. Maeda, S. Nagase, T. Akasaka, N. Kobayashi, Phys. Chem. Chem. Phys. 15 (2013) 3593.
[22] P. Štěpánek, P. Bouř, J. Comput. Chem. 36 (2015) 723.
[23] J. Tomasi, B. Mennucci, R. Cammi, Chem. Rev. 105 (2005) 2999.
[24] M.J. Frisch, G.W. Trucks, H.B. Schlegel, G.E. Scuseria, M.A. Robb, J.R. Cheeseman, G. Scalmani, V. Barone, B. Mennucci, G.A. Petersson, H. Nakatsuji, M. Caricato, X. Li, H.P. Hratchian, A.F. Izmaylov, J. Bloino, G. Zheng, J.L. Sonnenberg, M. Hada, M. Ehara, K. Toyota, R. Fukuda, J. Hasegawa, M. Ishida, T. Nakajima, Y. Honda, O. Kitao, H. Nakai, T. Vreven, J.A. Montgomery, J.E. Peralta, F. Ogliaro, M. Bearpark, J.J. Heyd, E. Brothers, K.N. Kudin, V.N. Staroverov, R. Kobayashi, J. Normand, K. Raghavachari, A. Rendell, J.C. Burant, S.S. Iyengar, J. Tomasi, M. Cossi, N. Rega, J.M. Millam, M. Klene, J.E. Knox, J.B. Cross, V. Bakken, C. Adamo, J. Jaramillo, R. Gomperts, R.E. Stratmann, O. Yazyev, A.J. Austin, R. Cammi, C. Pomelli, J.W. Ochterski, R.L. Martin, K. Morokuma, V.G. Zakrzewski, G.A. Voth, P. Salvador, J.J. Dannenberg, S. Dapprich, A.D. Daniels, Ö. Farkas, J.B. Foresman, J.V. Ortiz, J. Cioslowski, D.J. Fox, Gaussian 09, Revision D.01, Wallingford, CT, 2009.
[25] R. Ahlrichs, M. Baer, M. Haeser, H. Horn, C. Koelmel, Chem. Phys. Lett. 162 (1989) 165.
[26] F. Furche, R. Ahlrichs, J. Chem. Phys. 116 (2002) 7433.
[27] C. Angeli, K.L. Bak, V. Bakken, O. Christiansen, R. Cimiraglia, S. Coriani, P. Dahle, E.K. Dalskov, T. Enevoldsen, B. Fernandez, C. Haettig, K. Hald, A. Halkier, H. Heiberg, T. Helgaker, H. Hettema, H.J.A. Jensen, D. Jonsson, P. Joergensen, S. Kirpekar, W. Klopper, R. Kobayashi, H. Koch, O.B. Lutnaes, K.V. Mikkelsen, P. Norman, J. Olsen, M.J. Packer, T.B. Pedersen, Z. Rinkevicius, E. Rudberg, T.A. Ruden, K. Ruud, P. Salek, A. Sanchez de Meras, T. Saue, S.P.A. Sauer, B. Schimmelpfennig, K.O. Sylvester-Hvid, P.R. Taylor, O. Vahtras, D.J. Wilson, H. Agren, Dalton 2011, A Molecular Electronic Structure Program, University of Oslo, Oslo, 2005–2009.
[28] Z. Gasyna, P.N. Schatz, J.P. Hare, T.J. Dennis, H.W. Kroto, R. Taylor, D.R.M. Walton, Chem. Phys. Lett. 183 (1991) 283.
[29] P.J. Stephens, J. Chem. Phys. 52 (1970) 3489.
[30] T. Fahleson, J. Kauczor, P. Norman, S. Coriani, Mol. Phys. 111 (2013) 1401.
[31] T. Yanai, D. Tew, N.C. Handy, Chem. Phys. Lett. 393 (2004) 51.
[32] D. Padula, D. Picconi, A. Lami, G. Pescitelli, F. Santoro, J. Phys. Chem. A 117 (2013) 3355.
[33] N. Lin, H. Solheim, X. Zhao, F. Santoro, K. Ruud, J. Chem. Theory Comput. 9 (2013) 1557.